Appl Microbiol Biotechnol (2015) 99:2405–2418
DOI 10.1007/s00253-014-6127-3

ENVIRONMENTAL BIOTECHNOLOGY

Effects of selenium oxyanions on the white-rot fungus *Phanerochaete chrysosporium*

Erika J. Espinosa-Ortiz · Graciela Gonzalez-Gil · Pascal E. Saikaly · Eric D. van Hullebusch · Piet N. L. Lens

Received: 21 July 2014 / Revised: 26 September 2014 / Accepted: 3 October 2014 / Published online: 24 October 2014
© Springer-Verlag Berlin Heidelberg 2014

Abstract The ability of *Phanerochaete chrysosporium* to reduce the oxidized forms of selenium, selenate and selenite, and their effects on the growth, substrate consumption rate, and pellet morphology of the fungus were assessed. The effect of different operational parameters (pH, glucose, and selenium concentration) on the response of *P. chrysosporium* to selenium oxyanions was explored as well. This fungal species showed a high sensitivity to selenium, particularly selenite, which inhibited the fungal growth and substrate consumption when supplied at 10 mg L^{-1} in the growth medium, whereas selenate did not have such a strong influence on the fungus. Biological removal of selenite was achieved under semi-acidic conditions (pH 4.5) with about 40 % removal efficiency, whereas less than 10 % selenium removal was achieved for incubations with selenate. *P. chrysosporium* was found to be a selenium-reducing organism, capable of synthesizing elemental selenium from selenite but not from selenate. Analysis with transmission electron microscopy, electron energy loss spectroscopy, and a 3D reconstruction showed that elemental selenium was produced intracellularly as nanoparticles in the range of 30–400 nm. Furthermore, selenite influenced the pellet morphology of *P. chrysosporium* by reducing the size of the fungal pellets and inducing their compaction and smoothness.

Keywords Fungal pellets · Selenium removal · Selenium nanoparticles · *Phanerochaete chrysosporium*

Introduction

Selenium (Se) is well known for being both essential and toxic to human and animal life. As an essential biological trace element, the absence or deficiency in the human diet might cause major health issues (Rayman 2012). On the other hand, the toxicity of Se is only about one order of magnitude above its essential level (Fordyce 2013), leading to severe consequences for human health, from hair loss to dermal, respiratory, and neurological damages (USHHS 2003).

As a bulk material, Se has been used in a broad range of different applications, such as fertilizer, dietary supplement and fungicide, as well as in the glass and electronic industries. The extensive use and consumption of Se has raised plenty of concerns, since it was identified as a major threat for aquatic ecosystems in the 1980s (Hamilton 2004). Concentrations from a few to thousand of micrograms of Se per liter of the toxic, water-soluble oxyanions of Se, selenate (SeO_4^{2-}), and selenite (SeO_3^{2-}) are mainly found in the wastewater of industries associated to the production of glass, pigments, solar batteries and semiconductors, mining, refinery, coal combustion, petrochemical, thermal power stations, electronic, and agricultural activities (Lenz and Lens 2009; Soda and Ike 2011).

Traditionally, physicochemical methods have been used for the removal of Se oxyanions from water (Bleiman and Mishael 2010; Frankenberger et al. 2004; Geoffroy and Demopoulos 2011; Mavrov et al. 2006; Nguyen et al. 2005;

Electronic supplementary material The online version of this article (doi:10.1007/s00253-014-6127-3) contains supplementary material, which is available to authorized users.

E. J. Espinosa-Ortiz (✉) · G. Gonzalez-Gil · P. N. L. Lens
UNESCO-IHE Institute for Water Education, P.O. Box 3015, 2601 DA Delft, The Netherlands
e-mail: jime_na_es@yahoo.com.mx

G. Gonzalez-Gil · P. E. Saikaly
Water Desalination and Reuse Center, Division of Biological and Environmental Sciences and Engineering, King Abdullah University of Science and Technology, Thuwal 13955-69000, Saudi Arabia

E. D. van Hullebusch
Laboratoire Géomatériaux et Environnement (EA 4508), UPEM, Université Paris-Est, 77454 Marne-la-Vallée, France

Zelmanov and Semiat 2013). The use of biological processes is an attractive alternative, due to the ability of biological agents to reduce toxic Se species to elemental selenium (Se^0), a more stable and less toxic form of this element (Zhang et al. 2005, 2008). The synthesis of Se^0 in biological treatment systems is an added value, particularly when it is produced and recovered at the nano size range (<100 nm). Elemental selenium nanoparticles (nSe^0) possess unique semiconducting, photoelectric, and X-ray sensing properties, which makes them attractive for their use in photocells, semiconductor rectifiers, and photocopy machines, as well as antifungal, anticancer (Ahmad et al. 2010; van Cutsem et al. 1990), and therapeutic agents (Beheshti et al. 2013).

The synthesis of nSe^0 from Se oxyanions has been successfully achieved using bacteria (Zhang et al. 2011), fungi (Sarkar et al. 2011; Vetchinkina et al. 2013), and plant extracts (Mittal et al. 2013; Prasad et al. 2013). Even though bacteria are the preferred microorganisms for the production of nanoparticles, the use of fungi is also promising, due to the ease of handling and scale-up, as well as their ability to produce large amounts of enzymes and ability to survive at low pH. The capacity of fungi to act as nanofactories has already been shown for more than 30 different fungal species, which were able to synthesize diverse nanoparticles, including nAg, nAu, $nTiO_2$, and nPt (Castro-Longoria et al. 2011; Rajakumar et al. 2012; Syed and Ahmad 2012; Verma et al. 2010). Although some fungal strains have been found to be selenium-reducing organisms, the synthesis of nSe^0 has only been demonstrated by two fungal species, *Alternaria alternata* (Sarkar et al. 2011) and *Lentinula edodes* (Vetchinkina et al. 2013).

There has been some research on the metabolism of Se in filamentous fungi, including uptake and volatilization (Barkes and Fleming 1974; Fleming and Alexander 1972; Gharieb et al. 1995; Tweedie and Segel 1970; Ramadan et al. 1988); however, the information is still scarce. The limited knowledge regarding Se–fungi interactions hampers the full exploitation of fungi in Se remediation technologies and as nSe^0producing agents. Further investigations are required to elucidate the influence of Se on fungal morphology, growth, and ability to synthesize nSe^0.

White-rot fungi are well known for their unique ability to generate ligninolytic enzymes (i.e., lignin peroxidase, manganese peroxidase, laccase), which makes them attractive for the degradation of a wide range of hazardous compounds (Cameron et al. 2000; Lee et al. 2014), as well as for the synthesis of different nanoparticles (e.g., nAg, Chan and Don 2013; Vigneshwaran et al. 2006). The capacity of the white-rot fungus *Phanerochaete chrysosporium* to degrade organic compounds has been demonstrated (Moldes et al. 2003; Wang et al. 2009), as well as its ability to synthesize metal (Ag and Au) nanoparticles (Sanghi et al. 2011; Vigneshwaran et al. 2006). This fungus is able to self-immobilize in the form of pellets, which has many practical advantages over dispersed mycelial growth (Pazouki and Panda 2000; Thongchul and Yang 2003).

The aim of this study was to explore the potential of *P. chrysosporium* as a selenium-reducing organism to treat effluents polluted with Se oxyanions and to enlarge the scope of biological agents for the mycosynthesis of nanomaterials. Specifically, the influence of glucose concentration, pH, and Se oxyanion concentration on the biomass growth, pelletization, and selenium removal efficiency was investigated. Transmission electron microscopy (TEM) images and 3D reconstruction were used to localize the synthesized nSe^0.

Materials and methods

Fungal culture and medium composition

The fungal strain *P. chrysosporium* (MTCC 787) was obtained from the Institute of Microbial Technology (IMTECH), Chandigarh (India). The fungus was grown on malt agar plates at 37 °C for 3 days. Subcultures were routinely prepared as required and were maintained at 4 °C. A fungal spore solution was prepared by harvesting all the fungal spores from one of the 3-day-old agar plates into 50 mL of nitrogen-limited liquid medium. Fungi were grown in 100-mL Erlenmeyer flasks with 50 mL of medium. The flasks were inoculated with 2 % (*v*/*v*) of the spore suspension and incubated at 30 °C on a rotating orbital incubator shaker (Innova 2100, New Brunswick Scientific) set at 150 rpm. Subcultures of the 2-day-old fungal growth in the flasks were used as the final inoculum (2 % *v*/*v*, 0.003 g dry biomass L^{-1}). The use of a 2-day fungal growth as inoculum instead of a spore solution was found to be more efficient in terms of maintaining a reproducible formation and shape of fungal pellets. Furthermore, this approach allowed quantifying, by dry weight, the amount of biomass used as inoculum for the experiments.

The nitrogen-limited liquid medium was composed of the following (g L^{-1}): glucose, 10; KH_2PO_4, 2; $MgSO_4 \cdot 7H_2O$, 0.5; NH_4Cl, 0.1; $CaCl_2 \cdot 2H_2O$, 0.1; thiamine, 0.001; and 5 mL of trace element solution (Tien and Kirk 1988). After adjusting the pH to 4.5, the medium was sterilized at 123 kPa and 110 °C for 30 min and cooled to room temperature before use.

Batch experiments

Fungal interaction with selenate and selenite

The effect of SeO_4^{2-} and SeO_3^{2-} on the morphology and growth of *P. chrysosporium* was assessed in batch incubations. Fungal pellets were formed and grown in the presence of either Na_2SeO_4 or Na_2SeO_3 (10 mg Se L^{-1}) for 12 days. Abiotic controls without biomass and with dead biomass

(autoclaved at 121 °C, 123 kPa) were included to account for potential abiotic reactions and potential adsorption of Se to inert biomass, respectively. Biotic controls, in which the fungus was grown in the absence of Se, were used to record growth characteristics under non-stressful conditions. In order to avoid contamination and to maintain axenic growth of the fungus, experimental flasks were sacrificed after each sampling step for analysis (t=0, 1, 2, 3, 4, 8, and 12 days). All incubations were conducted in triplicates.

Effect of operational parameters on fungal growth, pelletization, and Se removal

Batch experiments were conducted to examine the effect of solution pH (2.5–7.0), concentration of glucose (0.5–10 g L^{-1}), and initial concentration of Se (2–10 mg Se L^{-1}) added as SeO_3^{2-} or SeO_4^{2-} on the removal of total soluble Se. To assess the effect of pH, the medium pH was adjusted by adding 0.1 M KOH or 0.1 M HCl at the beginning of the experiment and not controlled afterwards. All experiments were conducted under the same conditions as above, varying one operational parameter at a time and keeping the others constant. The incubation period for these experiments was 4 days, which was observed to be the period at which most of the biomass was already produced.

TEM and electron energy loss spectroscopy (EELS) analysis

Fixed (glutaraldehyde 2.5 % in phosphate-buffered saline, pH 7) fungal samples were placed on a carbon-coated copper grid and stained with 0.5 % uranyl acetate (Burghardt and Droleskey 2006). Imaging of samples was performed on a Titan G2 80–300-kV transmission electron microscope (FEI Company, The Netherlands) equipped with a 4 k×4 k charge-coupled device (CCD) camera model US4000 and an energy filter model GIF Tridiem (Gatan, Inc.). The general morphology and size of the produced Se^0 particles were determined using TEM images. Particle size measurements were done using ImageJ software (version 1.47, National Institutes of Health, USA) (Rasband 1997–2014) based on TEM images. The average particle size was calculated from measuring particles in random fields of view (Teodoro et al. 2011). To obtain the map distribution of selenium in the samples, the EELS signal from selenium L edge (Se-L edge of 1,436 eV) and M edge (Se-M edge of 57 eV) was acquired in energy-filtered TEM (EFTEM) mode. Each elemental map was created by using a three-window method (Kim and Dong 2011).

To determine the location of the Se^0 particles within the fungal biomass, a 3D reconstruction was done. The sample was imaged using a Titan CT operating at 300 kV equipped with a 4 k CCD camera (Gatan, Pleasanton, CA, USA). Tilt series for tomographic reconstruction were acquired using the Xplore 3D tomography software (FEI Company). Using a tilt range of ±68°, images were captured using a Saxton scheme at 2° intervals (Koning and Koster 2013). The tomogram was generated using the Weighted-Back Projection algorithm as implemented in the IMOD software (Kremer et al. 1996). Segmentation and 3D rendering of the tomographic images was conducted using Avizo (Visualization Science Group) image-processing software.

Analytical methods

After the incubation period, samples were centrifuged at 6,000 rpm for 15 min. The supernatant was used for measuring the chemical oxygen demand (COD), glucose, and the total soluble residual Se concentration in solution. The COD was determined according to the APHA 5220D standard procedure (APHA 1995). The glucose concentration was analyzed with the dinitrosalicylic acid method using D-glucose as standard (Miller 1959). For the measurement of the total Se concentration, the samples were further filtered (0.45 μm) and preserved with an acidified solution of 0.5 % HNO_3 in ultrapure water (Milli-Q water, 18 MΩ cm). Selenium was analyzed by inductively coupled plasma spectrometry (ICP-MS), with H_2/He (7:93) as the reaction gas, and ^{78}Se and ^{80}Se were used for quantification and verification, respectively. Lithium, gallium, scandium, rhodium, and iridium were used as internal standards. Samples were injected in 1:1 ratio and measured three times. The system was flushed entirely with an acidified solution (0.5 % HNO_3 in Milli-Q water).

After centrifugation, the fungal biomass was collected and washed several times with ultrapure water (Milli-Q). The biomass concentration was determined gravimetrically as dry weight by filtering the biomass suspension through a pre-dried (24 h at 105 °C) and pre-weighted filter paper (type GF/F, Whatman Inc., Florham Park, NJ) of 0.45-μm pore size. To count the number of pellets, samples were taken from the Erlenmeyer flasks after the incubation period and transferred manually into Petri dishes. The average size of the pellets was estimated with a Vernier caliper.

Results

Fungal interaction with selenium oxyanions

The presence of selenium oxyanions in the culture medium caused different effects on the growth, substrate consumption, and pellet morphology of *P. chrysosporium* after 12 days of incubation. The biomass yield was clearly reduced in incubations with SeO_3^{2-} in comparison to incubations with SeO_4^{2-} and the biotic control (Table 1). The addition of SeO_3^{2-} at 10 mg Se L^{-1} inhibited the fungal growth and resulted in an 80 % decrease of the biomass concentration compared to the

Table 1 Effects of selenium oxyanions on the fungal growth and morphology of *P. chrysosporium* over 12 days of incubation

Incubation	Shape	Surface	Color	Dry weight (g L^{-1})[a]	$Y_{x/s}$ (g g^{-1})[a, b]
Control	Pellet	Hairy	Ivory white	1.51±0.04	0.23±0.005
SeO_3^{2-}	Pellet	Smooth	Red-orange	0.27±0.05	0.11±0.04
SeO_4^{2-}	Pellet	Hairy and smooth	Ivory white	1.12±0.04	0.21±0.01

[a] Values are means (n=3) with standard deviations

[b] Biomass yield, calculated as $Y_{x/s} = \frac{\Delta x}{\Delta S}$

Se-free incubations (Fig. 1a). In contrast, SeO_4^{2-} was less inhibitory than SeO_3^{2-} to the fungal growth. In the presence of SeO_4^{2-} at 10 mg Se L^{-1}, a 30 % decrease of the biomass concentration compared to the biotic control was observed (Fig. 1a).

Substrate consumption was also decreased in the presence of SeO_3^{2-}, only about 30 % of the glucose was consumed (Fig. 1b). In the presence of SeO_4^{2-} and when Se oxyanions were omitted (i.e., biotic control), the glucose consumption was between 55 and 65 % (Fig. 1b). For all incubations, the pH was between 3.0 and 3.4 after the second day of incubation (Fig. 1c). The removal of Se (Fig. 1d) from the growth medium was higher for the SeO_3^{2-} incubation (40 % removal) compared to the SeO_4^{2-} incubation (<10 % removal). The abiotic controls (no biomass) did not show any changes from the initial conditions over 12 days of incubation (data not shown), indicating that the observed changes in the Se removal were due to the metabolic activity of *P. chrysosporium*. Moreover, no change in the Se concentration was observed for controls with dead biomass after the incubation period, which suggests that the decrease of the Se concentration with live biomass was not attributed to adsorption (data not shown). Incubations with SeO_3^{2-} presented a garlic like-odor, suggesting the formation of volatile forms of Se (Gharieb et al. 1995).

The morphology of the fungal pellets differed between incubations (Table 1 and Fig. 2). The formation of fungal pellets was observed in all the incubations (except for the dead control) irrespective of the presence or absence of Se. However, when exposed to SeO_3^{2-}, pellets of *P. chrysosporium* were compact and smooth, with a characteristic red-orange color, which indicates the reduction of SeO_3^{2-} to Se^0 (Gharieb et al. 1995; Sarkar et al. 2011). The number of pellets per incubation (<18) was lower, and the size of the pellets was in average smaller for the SeO_3^{2-} incubations (Fig. 2) compared to the other incubations. The morphology of pellets with SeO_4^{2-} was irregular, showing both smooth and hairy pellets, with an ivory white color (Fig. 2). In contrast, the pellets grown in the absence of Se were hairy, fluffy, and with an ivory white color, as reported before for this fungus (Huang et al. 2010). The number of pellets (>25) was higher, and their size was larger (Fig. 2) for the biotic control (Se-free incubations). It is important to highlight that reproducibility of fungal pelletization in the presence of SeO_3^{2-} was achieved in all the experiments.

The reduction of Se oxyanions to Se^0 was indicated by visualization and further confirmed by microscopic imaging. A red-orange coloration, suggesting the formation of Se^0, was only observed when the fungus was exposed to SeO_3^{2-}. Confirmation of the production of Se^0 particles by the fungal biomass was obtained with TEM-EELS analysis. From TEM imaging, Se^0 particles were not equally distributed in the hyphae (Fig. 3a–c), suggesting that Se^0 formation is specifically localized. Image analysis showed different size diameters for the produced particles, in a range of 35–400 nm, with the majority (>60 %) of the structures being *true* nanoparticles (<100 nm). A 3D reconstruction (Fig. 4) using a series of TEM images confirmed that the Se^0 particles were located within the fungal biomass (see Video S1 in supplementary material).

Effect of glucose concentration

The biomass growth of *P. chrysosporium* was more abundant at higher glucose concentrations for all incubations. Minimal fungal biomass was produced when using the lowest glucose concentration (0.5 g L^{-1}) for all incubations with and without selenium (Fig. 5).

P. chrysosporium showed a higher sensitivity to SeO_3^{2-} than to SeO_4^{2-} regardless of the glucose concentration used in the growth medium. A low biomass production along with a decrease of glucose consumption was observed for SeO_3^{2-} incubations compared to other treatments (Fig. 5). The biomass yield of SeO_3^{2-} incubations was in all cases less than 60 % compared to Se-free incubations (Table 2). Regardless of the glucose concentration, SeO_3^{2-} reduction to Se^0 was observed; pellets were smooth and with a red-orange color characteristic to the synthesis of Se^0. In the case of SeO_4^{2-}, the lack of coloration in the pellets suggests that SeO_4^{2-} is not reduced to Se^0. The removal of total soluble Se for SeO_3^{2-} incubations was higher at higher glucose concentrations (Fig. 6a), with a maximal Se removal efficiency (52 %) at glucose concentrations exceeding 7.5 g L^{-1}. However, Se removal for SeO_4^{2-} incubations barely occurred (<10 %) regardless of the glucose concentration (Fig. 6b). The fungal

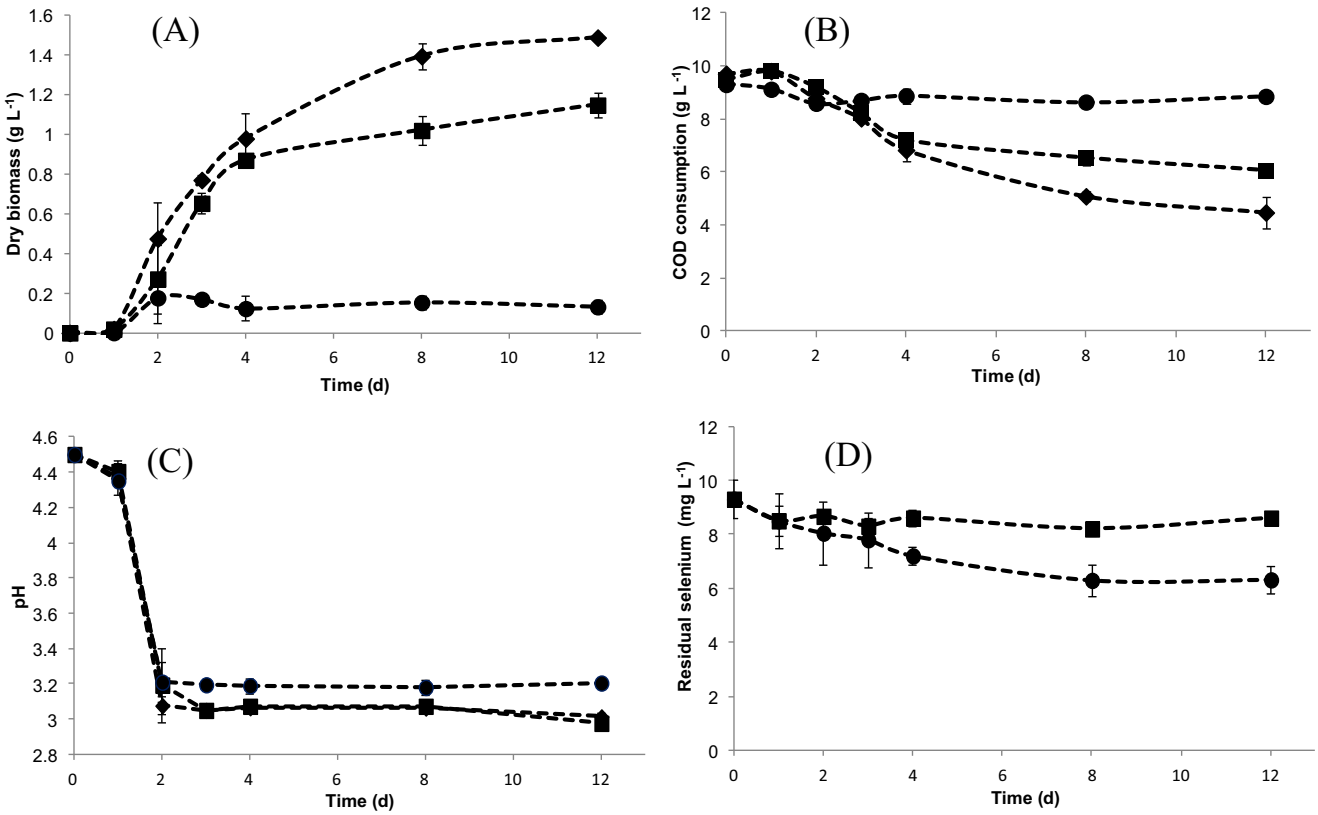

Fig. 1 **a** Growth of biomass in the biotic control (Se-free) or exposed to selenate and selenite (10 mg Se L^{-1}). **b** COD consumption. **c** pH profile. **d** Selenium removal. The symbols refer to: ◆ control, ■ SeO_4^{2-}, ● SeO_3^{2-}

pellet morphology at all glucose concentrations investigated and with addition of SeO_3^{2-} or SeO_4^{2-} showed the same characteristics as described in Table 1.

Effect of pH

When the fungi were grown at different initial pH values, the maximal biomass growth occurred at pH 4.5 for all the incubations (Fig. 7a). In general, the production of biomass was strongly inhibited under the most acidic conditions. At pH 2.5, there was about 70 % less biomass produced for the SeO_4^{2-} and Se-free incubations and about 90 % less biomass for SeO_3^{2-} compared to the maximum biomass growth obtained at pH 4.5 (Fig. 7a). At pH 3.0, a slight decrease in biomass concentration was found for SeO_4^{2-} and Se-free incubations compared to pH 4.5, whereas for SeO_3^{2-}, fungal

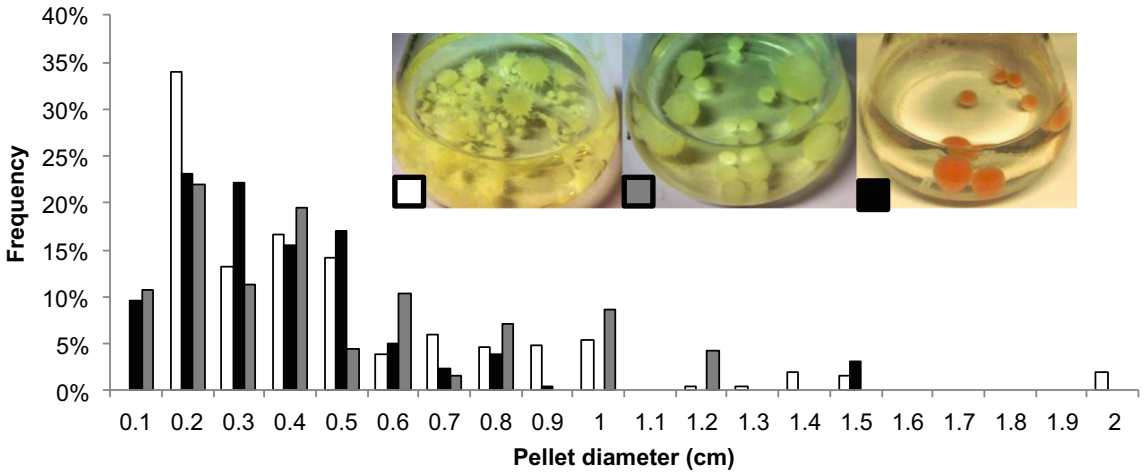

Fig. 2 Appearance and size distribution of pellets of *P. chrysosporium* produced in the absence of selenium (▣ control), with 10 mg L^{-1} of selenate (□ SeO_4^{2-}) or selenite (■ SeO_3^{2-}) after 12 days of incubation

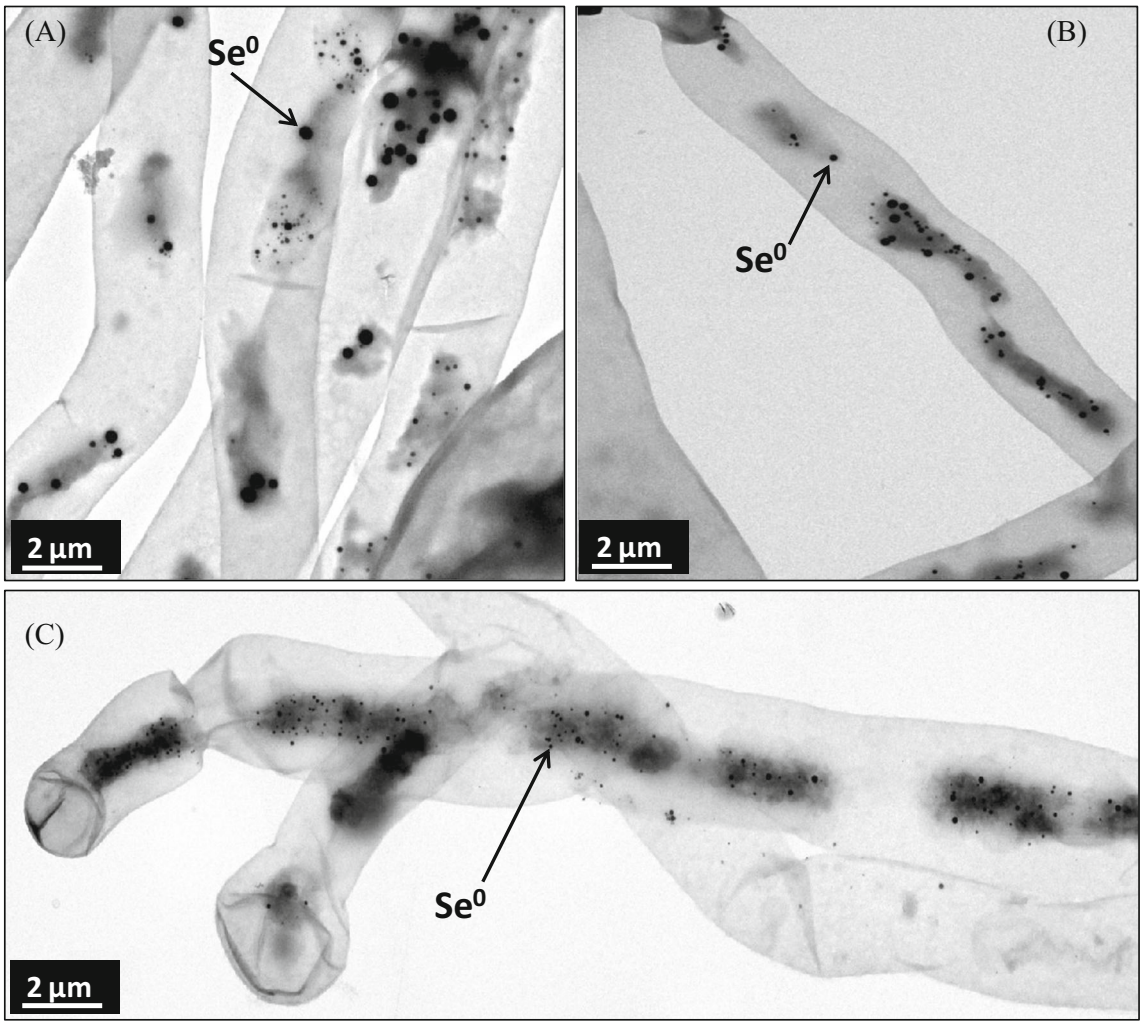

Fig. 3 Transmission electron micrographs of elemental selenium nanoparticles produced in the biomass of *P. chrysosporium*. **a** Distribution of Se^0 particles of different sizes within fungal biomass. **b**, **c** Localization of Se^0 particles within fungal biomass

growth was similarly inhibited as when grown at pH 2.5. For all incubations, biomass yields obtained at pH 7.0 were similar to those obtained at pH 4.5 (Table 2).

The formation of Se^0 was not observed for any of the SeO_4^{2-} incubations at different pH conditions (Fig. 7b). In contrast, the reduction of SeO_3^{2-} to Se^0 occurred over the whole pH range investigated (2.5–7.0). However, the removal of SeO_3^{2-} was pH dependent (Fig. 7b): under the most acidic conditions (pH 2.5–3.0), the percentage of Se removal was only 10 %, whereas at pH 4.5 and 7.0, the Se removal efficiency was about 45 %.

The growth of the fungus under different pH conditions leads to morphological changes of the growing mycelium (Fig. 8). Mycelia from Se-free media grown at low pH (2.5 and 3) exhibited an irregular short-strip shape as well as pellets, whereas regular mycelial pellets were observed at pH 4.5 and 7.0. The mycelia cultivated in the presence of SeO_3^{2-} showed less red-orange coloration at low pH (2.5 and 3.0) compared with those grown at pH 4.5 and 7.0. During incubations at pH 2.5, some pellets did even not show any sign of red-orange coloration, which indicated that the reduction of SeO_3^{2-} to Se^0 was limited. Incubations with SeO_4^{2-} only showed a sign of perturbation at pH 7.0, forming pellets and clumps of rough surface (Fig. 8).

Effects of selenium concentration

Fungal growth was inhibited with increasing Se concentrations, for both treatments with SeO_4^{2-} and SeO_3^{2-}. Compared to the Se-free incubations, the biomass concentration was reduced by 44–80 % at different doses of SeO_3^{2-} (Fig. 9a), whereas the biomass concentration was reduced by 11–24 % at increasing SeO_4^{2-} concentrations. The consumption of glucose was the highest for the incubations with lower Se concentrations (data not shown). The pH profile was similar for all the incubations, decreasing from initial pH 4.5 to 3.2±0.1.

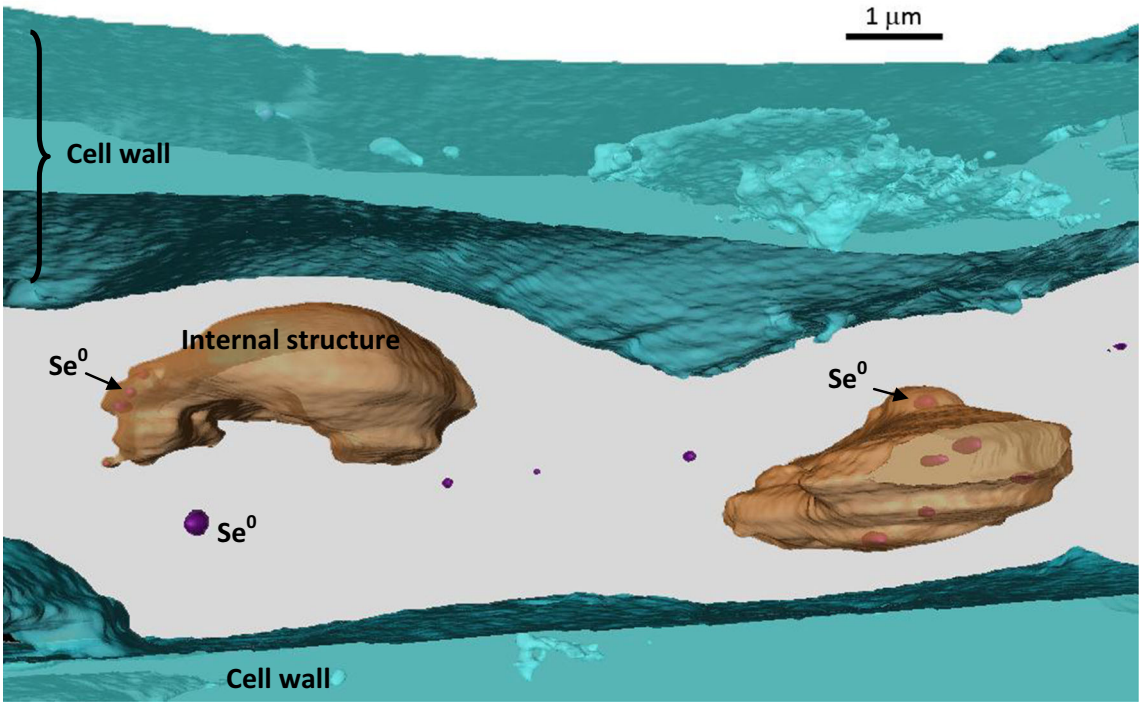

Fig. 4 3D reconstruction model of Se^0 nanoparticles within fungal biomass

The removal of Se oxyanions was not concentration dependent; it remained proportionally the same under all Se oxyanion concentrations tested (Fig. 9b). The removal efficiency of total soluble Se was about 10 and 40 % for incubations with SeO_4^{2-} and SeO_3^{2-}, respectively. No major morphological changes, in comparison to the already described characteristics (Table 1), were observed for the mycelia grown at different concentrations of SeO_3^{2-} or SeO_4^{2-}. Only, at low concentrations of SeO_3^{2-} (2–4 mg L^{-1}), a less intense red-orange coloration in the pellets was observed (data not shown).

Discussion

Inhibition of fungal growth induced by selenium oxyanions

The sensitivity of *P. chrysosporium* to Se in terms of dry biomass production was the highest when Se was added in the form of SeO_3^{2-}. A clear inhibitory effect of the fungal growth was observed even at SeO_3^{2-} concentrations as low as 2 mg Se L^{-1}. The inhibitory effect of SeO_3^{2-} to the fungal growth of filamentous, polymorphic, and unicellular fungi has been demonstrated before (Gharieb et al. 1995). Addition of

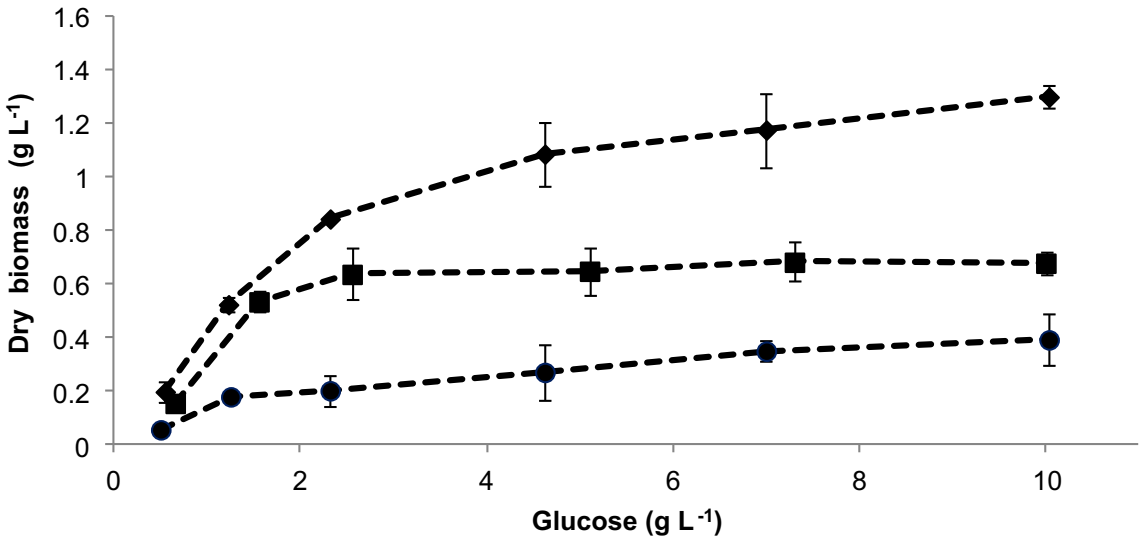

Fig. 5 Biomass growth of *P. chrysosporium* as a function of initial glucose concentrations and exposed to selenate or selenite (10 mg Se L^{-1}). Symbols refer to: ◆ control, ■ SeO_4^{2-}, and ● SeO_3^{2-}

Table 2 Yield of *P. chrysosporium* under different operational parameters over 4 days of incubation

Biomass yield ($Y_{x/s}$, g g^{-1})

Glucose (g L^{-1})	Control	SeO_3^{2-}	SeO_4^{2-}	pH	Control	SeO_3^{2-}	SeO_4^{2-}	Selenium (mg L^{-1})	SeO_3^{2-}	SeO_4^{2-}
0.5	0.45±0.09	0.20±0.03	0.30±0.03	2.5	0.15±0.02	0.14±0.06	0.16±0.03	2	0.25±0.02	0.36±0.03
1.5	0.46±0.02	0.26±0.06	0.41±0.01	3	0.27±0.04	0.10±0.02	0.24±0.05	4	0.20±0.02	0.36±0.03
2.5	0.39±0.01	0.20±0.04	0.34±0.01	4.5	0.33±0.05	0.20±0.04	0.28±0.08	6	0.19±0.05	0.35±0.01
5	0.37±0.04	0.20±0.04	0.32±0.07	7	0.32±0.03	0.16±0.05	0.26±0.02	8	0.25±0.04	0.35±0.01
7.5	0.34±0.01	0.23±0.09	0.31±0.04					10	0.21±0.05	0.34±0.02
10	0.27±0.01	0.15±0.04	0.25±0.02							
Conditions for this experiment: pH 4.5, 10 mg Se L^{-1}				Conditions for this experiment: Glucose 10 g L^{-1}, 10 mg Se L^{-1}				Conditions for this experiment: Glucose 10 g L^{-1}, pH 4.5		

SeO_4^{2-}, which is the least toxic Se oxyanion on an acute basis (Brix et al. 2001; Canton 1999), caused a less inhibitory effect on the fungal growth. In agreement with the results of the present study, previous investigations showed that the addition of SeO_4^{2-} had less impact on the inhibition of the growth of other white-rot fungi, such as *Bjerkandera adusta* (Catal et al. 2008), in comparison to SeO_3^{2-}. However, fungal tolerance to selenium oxyanions is species dependent (Gharieb et al. 1995). The growth of *Fusarium* sp., a selenium-reducing fungus, was more inhibited in the presence of SeO_4^{2-} than in the presence of SeO_3^{2-} (Gharieb et al. 1995). In the case of *Pleurotus ostreatus*, 2.5 mg L^{-1} of SeO_3^{2-} stimulated the fungal growth of mycelium, whereas 5 mg L^{-1} was inhibitory (Serafin-Muñoz et al. 2006). The tolerance to selenium is attributed to the incapacity of fungi to distinguish between Se and S. It has been suggested that selenium toxicity is due to the incorporation of Se into sulfur-containing amino acids and proteins instead of sulfur, altering their structure and disrupting the enzyme activity (Golubev and Golubev 2002; Lauchli 1993).

The composition of the growth medium can also influence the tolerance to Se, and therefore the fungal growth, particularly the presence of a certain carbon source (e.g., glucose), sulfate, sulfur-containing amino acids, or glutamine (Golubev and Golubev 2002; Serafin-Muñoz et al. 2006). Glucose is the most readily utilizable substrate by fungi; it is of crucial importance for the optimal growth of fungi and it has been suggested to have an active role in SeO_3^{2-} uptake (Gharieb and Gadd 2004). As it has been demonstrated in previous studies (Kim et al. 2003), the variation of the initial glucose concentration in the medium has a noticeable effect on the growth of fungi and biomass yield (Table 2). Indeed, above 5 g L^{-1}, increasing the glucose concentration did not have a prominent effect on the fungal growth when SeO_3^{2-} was added to the medium (Fig. 5). The use of high concentrations of glucose (10 g L^{-1}) is common for the production of fungal biomass; however, such concentrations are not commonly found in wastewaters. A clear reduction of the glucose uptake was observed when *P. chrysosporium* was fed with selenium oxyanions (Fig. 1 and Table 1), particularly with SeO_3^{2-}, which indicates a decrease of the carbohydrate metabolism in the cells.

Increased concentrations of Se oxyanions in the growth media reduced the biomass production of *P. chrysosporium* (Fig. 9a). This is consistent with previous research conducted with other fungal strains (Ramadan et al. 1988). Similar effects have been observed for different fungal species exposed to heavy metals (Graz et al. 2011; Kim et al. 2003). The sensitivity of fungi to toxic elements (i.e., heavy metals) is species dependent, which is mainly attributed to different detoxification mechanisms utilized by various fungi (Kim et al. 2003). Fungal growth was also influenced by pH. In comparison to other microorganisms, it is well known that a low pH is favorable for the growth of fungi. This study showed that the maximal fungal growth of *P. chrysosporium* was achieved at pH 4.5 for all incubations with and without Se (Fig. 7a).

Morphological effects induced by selenium oxyanions

This study shows that the presence of SeO_3^{2-} in the growth medium of *P. chrysosporium* induces growth stress to this organism (Fig. 1a) which resulted in compact and smooth pellets of smaller diameter than pellets formed in the absence of SeO_3^{2-} (Fig. 2). Certain species of filamentous fungi are able to grow in the form of pellets under submerged conditions in the liquid medium. Pellets are usually formed as a result of the interaction between hyphae, solid particles, and spores (Prosser 1995). Even though the exact mechanism for fungal pelletization remains unclear, it is well known that pelletization is driven by cultivation conditions (e.g., pH, temperature, agitation rate), composition of the growth medium (e.g., carbon source, nutrients, additives, carriers), and inoculum (e.g., age and size of inoculum) (Metz and Kossen 1977; Papagianni 2004).

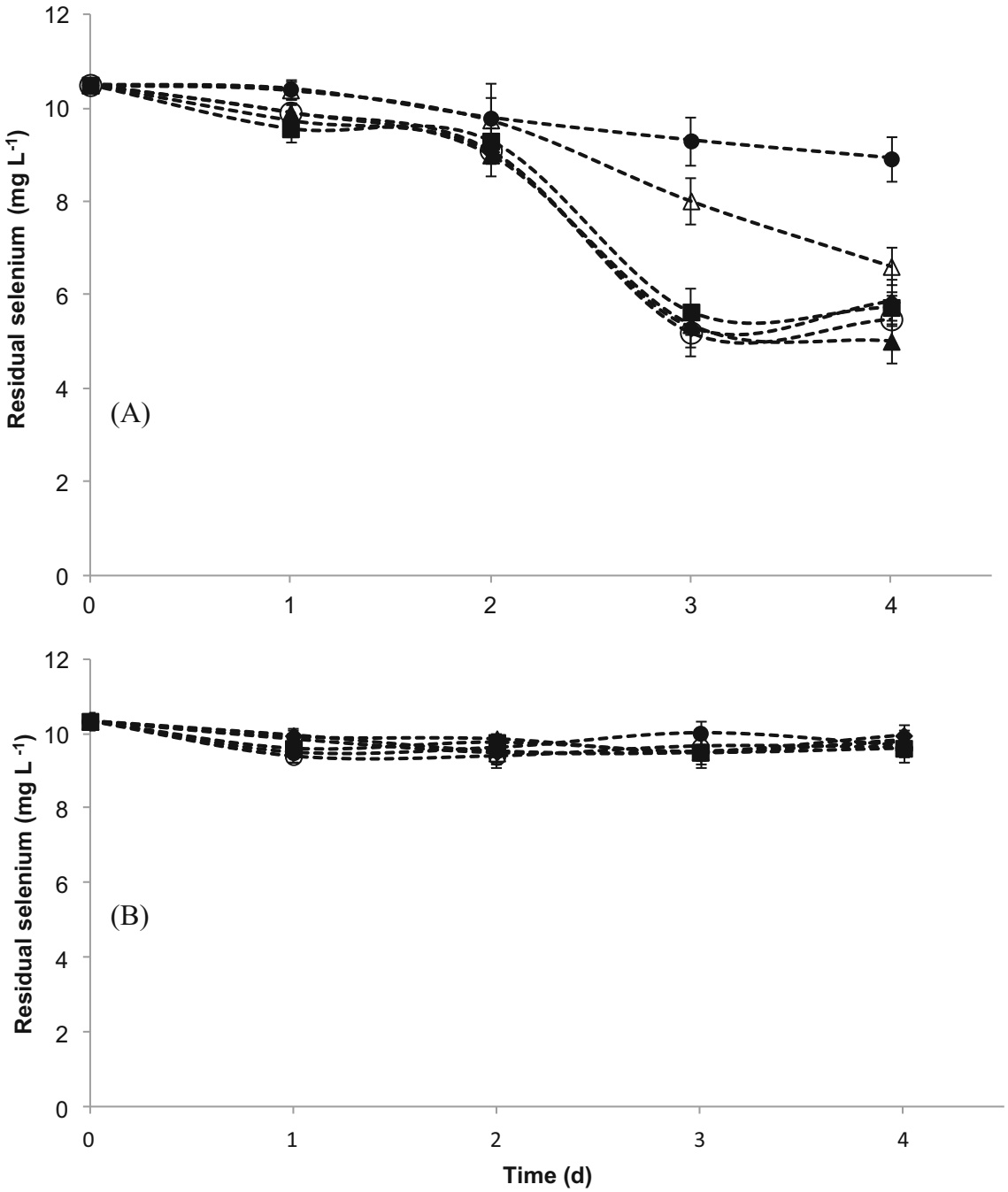

Fig. 6 Removal of selenium oxyanions (10 mg Se L^{-1}) at different glucose concentrations. **a** Selenite and **b** selenate incubations. Symbols refer to: ● 0.5, △ 1.5, ■ 2.5, ◆ 5, ○ 7.5, and ▲ 10 mg glucose L^{-1}

Self-immobilization of fungi as pellets seems to occur mainly under stressful conditions, such as limitation of nutrients or oxygen. The presence of toxic compounds also influences the formation and characteristics of the pellets. Saraswathy and Hallberg (2005) showed that the presence of pyrene in the growth medium resulted in the formation of pellets by two *Penicillium ochrochloron* strains, and the size and texture of the pellets formed varied for each individual strain.

Removal of selenium oxyanions by ***P. chrysosporium***

The present study demonstrates that *P. chrysosporium* possesses selenium-reducing capabilities. The main fungal species that are reported with selenium-reducing capabilities include *A. alternata* (Sarkar et al. 2011), *Aspergillus* spp. (Moss et al. 1987; Gharieb et al. 1995), *Fusarium* sp. (Ramadan et al. 1988; Gharieb et al. 1995), *Mortierella* spp. (Zieve et al. 1985), *Penicillium* spp. (Brady et al. 1996), and *L. edodes*

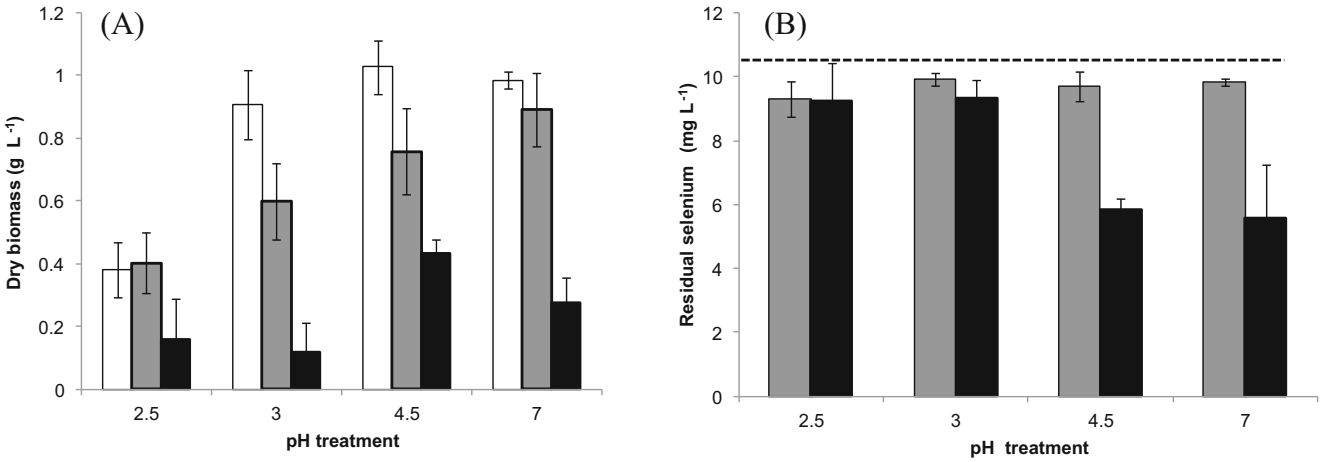

Fig. 7 Response of *P. chrysosporium* to selenium oxyanions under different pH conditions. **a** Production of fungal biomass (dry weight). **b** Selenium removal efficiency. Symbols refer to: □ control, ▩ SeO_4^{2-}, ■ SeO_3^{2-}, and – – – – initial Se concentration

(Vetchinkina et al. 2013). Selenium removal (40–50 %) by *P. chrysosporium* mainly occurred when supplied with SeO_3^{2-}. This can be attributed to SeO_3^{2-} reduction to Se^0 as a detoxification mechanism (Gharieb et al. 1995). Se tolerance and detoxification by fungi have been mainly ascribed to biomethylation of Se compounds, which involves the reduction of inorganic Se forms to less toxic and volatile derivatives, such as dimethylselenide (Gadd 1993), or the reduction of selenium oxyanions to elemental selenium, producing intra- or extracellular red-orange deposits of Se^0 (Gharieb et al. 1995). The detection of a garlic-like odor in SeO_3^{2-} incubations suggests that volatile Se compounds are formed during the reduction to Se^0 (Gharieb et al. 1995). Further research is required to quantify the volatile fraction and the speciation of selenium in the gas phase.

The detailed mechanism of selenate and selenite reduction by *P. chrysosporium* is not known. It has been reported that glutathione, a common intracellular reduced thiol in various organisms, including fungi, is involved in detoxification processes. A recent study showed that *P. chrysosporium* accumulated high levels of glutathione when exposed to high concentrations of heavy metals (Xu et al. 2014). It has been proposed that in some bacteria, selenite reacts with glutathione producing selenodiglutathione which is reduced by glutathione reductases to form a selenium persulfide compound. This compound then dismutates into Se^0 and reduced glutathione

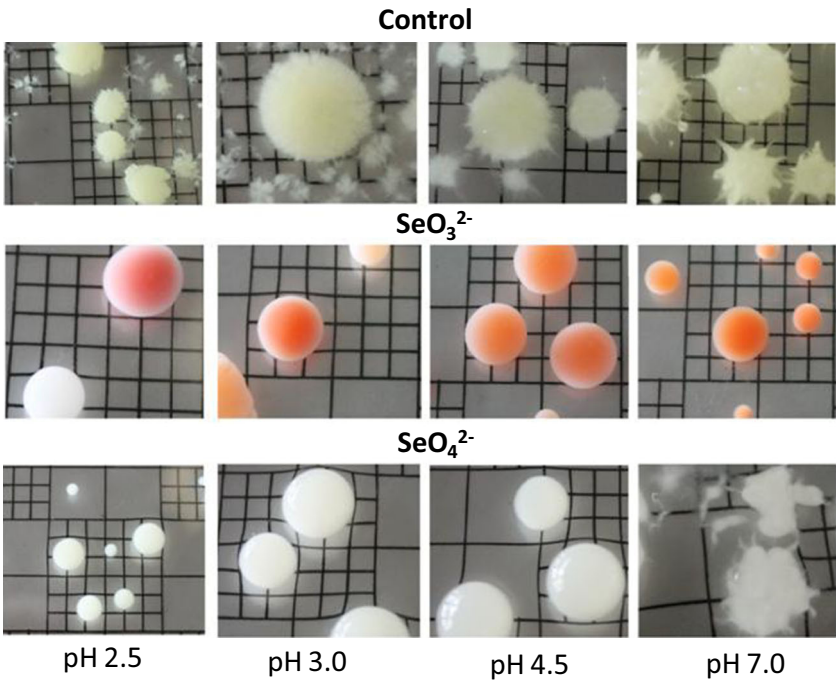

Fig. 8 Effect of growth medium pH on the morphology of *P. chrysosporium* pellets

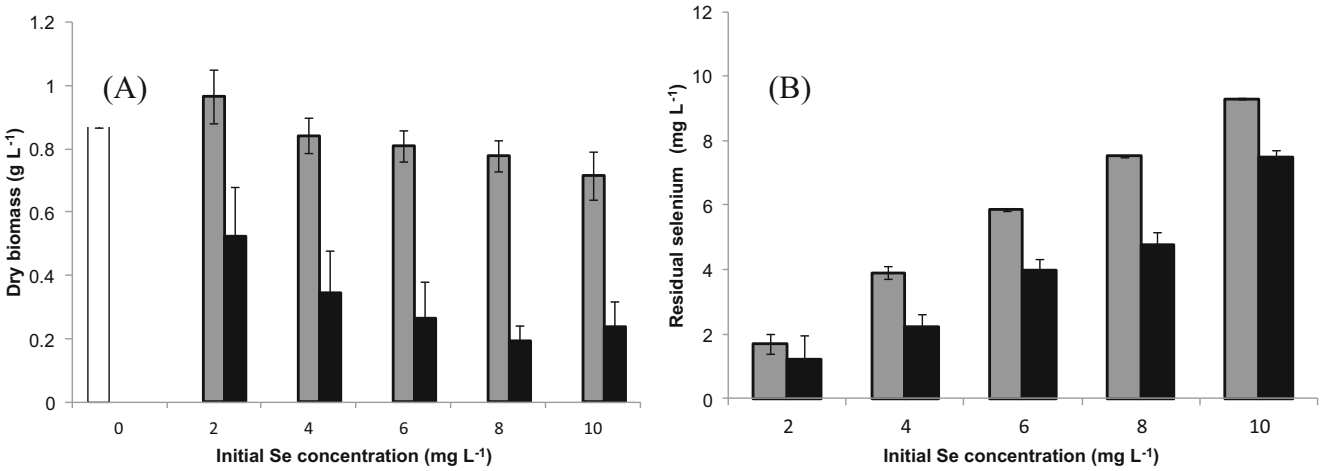

Fig. 9 Response of *P. chrysosporium* to different concentrations of selenium oxyanions. **a** Production of fungal biomass (dry weight). **b** Selenium removal efficiency. Symbols refer to: □ control, ▒ SeO_4^{2-}, ■ SeO_3^{2-}

(Debieux et al. 2011). It is possible that *P. chrysosporium* uses a similar glutathione-dependent mechanism for the reduction of selenite. However, further studies involving proteomics would be required to test this hypothesis and to determine the reductases involved in the formation of the Se^0 nanoparticles.

The removal of SeO_3^{2-} by *P. chrysosporium* was influenced by the glucose concentration. Glucose concentrations higher than 2.5 g L^{-1} showed maximal removal of this Se oxyanion. A previous study demonstrated the stimulatory effect of glucose addition on SeO_3^{2-} accumulation by the yeast *Saccharomyces cerevisiae*, suggesting a predominant role of the metabolic activity to transport SeO_3^{2-} by the cells (Gharieb and Gadd 2004). The positive influence of glucose on the uptake of SeO_3^{2-} has also been observed in bacteria, i.e., *Salmonella typhimurium* (Brown and Shrift 1980).

The pH also played an important role on the fungal removal of Se as SeO_3^{2-} (Fig. 7b). Similar maximum removal efficiencies of SeO_3^{2-} were obtained between pH 4.5 and 7.0, suggesting that the treatment of selenite-containing wastewater using fungi can be applied to both acidic and neutral waste streams. This feature represents a notable advantage over the reduction of SeO_3^{2-} to Se^0 by bacteria, since the bacterial process occurs at near to neutral up to alkaline pH (Lortie et al. 1992; Mishra et al. 2011).

Selenium removal was less than 10 % for SeO_4^{2-} incubations, regardless of the glucose concentration (Fig. 5), pH (Fig. 7a), or initial Se concentration (Fig. 9a). Therefore, the use of fungal pellets of *P. chrysosporium* to remove SeO_4^{2-} from wastewater is not recommended. The lack of red-orange coloration in the fungal biomass suggested that *P. chrysosporium* was not able to reduce SeO_4^{2-} to Se^0, as it has been reported also for other fungi (Vetchinkina et al. 2013). Even though the Se speciation was not determined in this study, the results suggest that the capacity of this fungus to reduce SeO_4^{2-} to SeO_3^{2-} is limited, as the overall soluble total selenium removal was less than 10 %. If this had been transformed into selenite, then selenite would have been further reduced to selenium nanoparticles (the fungus readily reduced selenite to selenium nanoparticles). However selenium nanoparticles were not detected in these incubations. Moreover, if the selenate had been transformed into selenite, then the fungal growth would have been inhibited similarly as for the incubations with selenite (Fig. 1a).

Production of Se^0 by *P. chrysosporium*

The characteristic orange-red coloration that results from Se^0 synthesis (Fig. 2) was only observed in the biomass of the SeO_3^{2-} incubations and not in the medium, indicating immobilization of Se^0 in the fungal material. Deposition and entrapment of Se^0 within fungal biomass might be advantageous for technical applications, considering that there will be no loss or washout of any material. Formation of *true* nanoparticles of Se^0 (particles of size <100 nm) was also observed (Fig. 3). The synthesis of Se^0 from SeO_3^{2-} by different bacterial strains such as *Bacillus megaterium*, *Sulfurospirillum barnesii*, and *Selenihalanaerobacter shriftii* has also been reported (Oremland et al. 2004; Mishra et al. 2011). However, most of the particles produced by bacteria are much larger in size (200–1,000 nm) compared to those produced by *P. chrysosporium* (35–400 nm).

TEM cell characterization and the corresponding 3D reconstruction (Fig. 4) confirmed that the majority of the Se^0 particles were located inside the fungal cells and that some were localized within the fungal cell wall, suggesting their intracellular formation. Mukherjee et al. (2001) suggested that intracellular production of nanoparticles is driven by the electrostatic interaction between the metal ions in solution and the enzymes in the fungal cell wall, binding on the fungal cell surface, where the metal ions are reduced, leading to the synthesis of nanoparticles that accumulate within the mycelia.

Even though the majority of the nanoparticles synthesized by fungi have been observed to be formed extracellularly (Verma et al. 2010; Syed and Ahmad 2012), a few species such as *Verticillium* sp. (Mukherjee et al. 2001; Sastry et al. 2003), *Thrichothecium* sp. (Ahmad et al. 2005), and *Aspergillus flavus* (Vigneshwaran et al. 2007; Rajakumar et al. 2012) synthesize nanoparticles intracellularly. From the TEM images (Fig. 3), it seems that the majority of nanoparticles are compartmentalized in the fungal cell, in intracellular structures. Further analyses need to be performed in order to determine specifically in which organelles or structures the synthesis of Se^0 is taking place. Some fungal species (*Aspergillus funiculosus* and *Fusarium* sp.) have shown the ability to compartmentalize elemental selenium in their vacuoles (Gharieb 1993; Gharieb et al. 1995), which have been suggested to regulate the uptake, detoxification, and tolerance to selenite in the yeast *S. cerevisiae*.

Potential applications

Removal of Se oxyanions at low pH is promising for the treatment of acidic effluents polluted with Se, particularly as SeO_3^{2-}. *P. chrysosporium* possesses the ability to intracellularly produce elemental selenium nanoparticles, which can be separated from the treated effluent in an immobilized form suitable for use in commercial applications. There is an increased interest in the use of nSe^0, including applications such as antifungal and anticancer agents (van Cutsem et al. 1990; Ahmad et al. 2010) as well as an effective agent to prevent and treat *Staphylococcus aureus* infections (Tran and Webster 2011). Besides, biogenic nSe^0 have been used for the production of high sensitivity sensors (Wang et al. 2010) and as potential affinity sorbents for contaminants such as mercury (Fellowes et al. 2011) and zinc (Jain et al. 2014). Moreover, the influence of Se (as SeO_3^{2-}) on the growth and pelletization of *P. chrysosporium* could be of potential application to control biomass growth in fungal bioreactors. Moreover, SeO_3^{2-} adds to the repertoire of factors that influence pellet formation and fungal morphology.

Acknowledgments The authors thank the EU for providing financial support through the Erasmus Mundus Joint Doctorate Programme ETeCoS^3 (Environmental Technologies for Contaminated Solids, Soils and Sediments, grant agreement FPA no. 2010-0009). This work was partly supported by a Global Research Partnership-Collaborative Fellows Award (GRFP-CF-2011-13-P) from the King Abdullah University of Science and Technology. The authors thank Rachid Sougrad for his assistance with TEM 3D image reconstruction.

Conflict of interest The authors declare that they have no conflict of interest.

References

Ahmad A, Senapati S, Khan MI, Kumar R, Sastry M (2005) Extra/intracellular, biosynthesis of gold nanoparticles by an alkalotolerant fungus, *Trichothecium* sp. J Biomed Nanotechnol 1:47–53. doi:10.1166/jbn.2005.012

Ahmad RS, Ali F, Gazal M, Parisa JF, Sassan R, Seyed MR (2010) Antifungal activity of biogenic selenium nanoparticles. World Appl Sci J 10(8):912–922

APHA (1995) Standard methods for water and wastewater examination, 19th edn. American Public Health Association, Washington

Barkes L, Fleming RW (1974) Production of dimethylselenide gas from inorganic selenium by eleven soil fungi. Bull Environ Contam Toxicol 12:308–311

Beheshti N, Soflaei S, Shakibaie M, Yazdi MH, Ghaffarifar F, Dalimi A, Shahverdi AR (2013) Efficacy of biogenic selenium nanoparticles against *Leishmania major*: in vitro and in vivo studies. J Trace Elem Med Biol 27(3):203–207. doi:10.1016/j.jtemb.2012.11.002

Bleiman N, Mishael YG (2010) Selenium removal from drinking water by adsorption to chitosan-clay composites and oxides: batch and columns tests. J Hazard Mat 183(1–3):590–595. doi:10.1016/j.jhazmat.2010.07.065

Brady JM, Tobin JM, Gadd GM (1996) Volatilization of selenite in aqueous medium by a *Penicillium* species. Mycol Res 100:955–961. doi:10.1016/S0953-7562(96)80048-7

Brix KV, Adams WJ, Reash RJ, Carlton RG, McIntyre DO (2001) Acute toxicity of sodium selenate to two daphnids and three amphipods. Environ Toxicol 16(2):142–150. doi:10.1002/tox.1018

Brown TA, Shrift A (1980) Assimilation of selenate and selenite by *Salmonella typhimurium*. Can J Microbiol 26:671–675

Burghardt RC, Droleskey R (2006) Transmission Electron Microscopy. Current Protocols in Microbiology. 3:2B.1.1–2B.1.39. doi:10.1002/9780471729259.mc02b01s03

Cameron MD, Timofeevski S, Aust SD (2000) Enzymology of *Phanerochaete chrysosporium* with respect to the degradation of recalcitrant compounds and xenobiotics. Appl Microbiol Biotechnol 54:751–758. doi:10.1007/s002530000459

Canton SP (1999) Acute aquatic life criteria for selenium. Environ Toxicol Chem 18:1425–1432. doi:10.1002/etc.5620180712

Castro-Longoria E, Vilchis-Nestor A, Avalos-Borja M (2011) Biosynthesis of silver, gold and bimetallic nanoparticles using the filamentous fungus *Neurospora crassa*. Colloids Surf B: Biointerfaces 83:42–48. doi:10.1016/j.colsurfb.2010.10.035

Catal T, Liu H, Bermek H (2008) Selenium induces manganese-dependent peroxidase production by the white-rot fungus *Bjerkandera adusta* (Willdenow) P. Karsten. Biol Trace Elem Res 123:211–217. doi:10.1007/s12011-007-8084-5

Chan YS, Don MM (2013) Biosynthesis and structural characterization of Ag nanoparticles from white-rot fungi. Mater Sci Eng C 33:282–288. doi:10.1016/j.msec.2012.08.041

Debieux CM, Dridge EJ, Mueller CM, Splatt P, Paszkiewicz K, Knight I, Florance H, Love J, Titball RW, Lewis RJ, Richardson DJ, Butler CS (2011) A bacterial process for selenium nanosphere assembly. Proc Natl Acad Sci U S A 108:13480–13485. doi:10.1073/pnas.1105959108

Fleming RW, Alexander M (1972) Dimethylselenide and dimethyltelluride formation by a strain of *Penicillium*. Appl Microbiol 24:424–429

Fordyce FM (2013) Selenium deficiency and toxicity in the environment. In: Selinus O (ed) Essentials of medical geology, revised edition. Springer, Netherlands, pp 375–416

Frankenberger WT, Amrhein C, Fan TWM, Flaschi D, Glater J, Kartinen E, Kovac K, Lee E, Ohlendorf HM, Owens L, Terry N, Toto A (2004) Advanced treatment technologies in the remediation of seleniferous drainage waters and sediments. Irrig Drain Syst 18:19–41. doi:10.1023/B:IRRI.0000019422.68706.59

Gadd GM (1993) Microbial formation and transformation of organometallic and organometalloid compounds. FEMS Microbiol Rev 11: 297–316. doi:10.1111/j.1574-6976.1993.tb00003.x

Gharieb MM (1993) Selenium toxicity, accumulation and metabolism by fungi and influence of the fungicide dithane. PhD thesis. University of Dundee

Gharieb MM, Gadd GM (2004) The kinetics of ^{75}[Se]-selenite uptake by *Saccharomyces cerevisiae* and the vacuolization response to high concentrations. Mycol Res 108(12):1415–1422. doi:10.1017/S0953756204001418

Gharieb MM, Wilkinson SC, Gadd GM (1995) Reduction of selenium oxyanions by unicellular, polymorphic and filamentous fungi: cellular location of reduced selenium and implication for tolerance. J Ind Microbiol 14(3–4):300–311. doi:10.1007/BF01569943

Geoffroy N, Demopoulos GP (2011) The elimination of selenium (IV) from aqueous solution by precipitation with sodium sulfide. J Hazard Mater 185(1):148–154. doi:10.1016/j.jhazmat.2010.09.009

Golubev VI, Golubev NV (2002) Selenium tolerance of yeasts. Microbiology 71(4):455–459. doi:10.1023/A:1019829107239

Graz M, Pawlikowska-Pawlega B, Jarosz-Wilkolazka A (2011) Growth inhibition and intracellular distribution of Pb ions by the white-rot fungus *Abortiporus biennis*. Int Biodeterior Biodegrad 65:124–129. doi:10.1016/j.ibiod.2010.08.010

Fellowes JW, Pattrick RA, Green DI, Dent A, Lloyd JR, Pearce CI (2011) Use of biogenic and abiotic elemental selenium nanospheres to sequester elemental mercury released from mercury contaminated museum specimens. J Hazard Mater 189(3):660–669. doi:10.1016/j.jhazmat.2011.01.079

Hamilton SJ (2004) Review of selenium toxicity in the aquatic food chain. Sci Total Environ 326(1–3):1–31. doi:10.1016/j.scitotenv.2004.01.019

Huang DL, Zeng GM, Feng CL, Hu S, Zhao MH, Lai C, Zhang Y, Jiang XY, Liu HL (2010) Mycelial growth and solid-state fermentation of lignocellulosic waste by white-rot fungus *Phanerochaete chrysosporium* under lead stress. Chemosphere 81:1091–1097. doi:10.1016/j.chemosphere.2010.09.029

Jain R, Jordan N, Schild, van Hullebusch ED, Weiss S, Franzen C, Farges F, Hübner R, Lens PNL (2014) Adsorption of zinc by biogenic elemental selenium nanoparticles. Chem Eng J. doi:10.1016/j.cej.2014.09.057

Kim J, Dong H (2011) Application of electron energy-loss spectroscopy (EELS) and energy-filtered transmission electron microscopy (EFTEM) to the study of mineral transformation associated with microbial Fe-reduction of magnetite. Clays Clay Miner 59:176–188. doi:10.1346/CCMN.2011.0590206

Kim CG, Power SA, Bell JNB (2003) Effects of cadmium on growth and glucose utilization of ectomycorrhizal fungi in vitro. Mycorrhiza 13: 223–226. doi:10.1007/s00572-003-0235-8

Koning R, Koster A (2013) Cellular nanoimaging by cryo electron tomography. In: Sousa AA, Kruhlak MJ (eds), Nanoimaging: Methods and Protocols 950. Humana Press, Totowa, NJ. pp. 227–251

Kremer JR, Mastronarde DN, McIntosh JR (1996) Computer visualization of three-dimensional image data using IMOD. J Struct Biol 116: 71–76. doi:10.1006/jsbi.1996.0013

Lauchli A (1993) Selenium in plants: uptake, functions and environmental toxicity. Bot Acta 106:455–468

Lee H, Jang Y, Choi YS, Kim MJ, Lee J, Lee H, Hong JH, Lee YM, Kim GH, Kim JJ (2014) Biotechnological procedures to select white rot fungi for the degradation of PAHs. J Microbiol Methods 97:56–62. doi:10.1016/j.mimet.2013.12.007

Lenz M, Lens PNL (2009) The essential toxin: the changing perception of selenium in environmental sciences. Sci Total Environ 407:3620–3633. doi:10.1016/j.scitotenv.2008.07.056

Lortie L, Gould WD, Rajan S, McCready RGL, Cheng KJ (1992) Reduction of selenate and selenite to elemental selenium by a *Pseudomonas stutzeri* isolate. Appl Environ Microbiol 58:4042–4044

Metz B, Kossen NWF (1977) The growth of molds in the form of pellets—a literature review. Biotechnol Bioeng 19:781–799. doi:10.1002/bit.260190602

Mavrov V, Stamenov S, Todorova E, Chmiel H, Erwe T (2006) New hybrid electrocoagulation membrane process for removing selenium from industrial wastewater. Desalination 201:290–296. doi:10.1016/j.desal.2006.06.005

Miller GL (1959) Use of dinitrosalicylic acid reagent for determination of reducing sugar. Anal Chem 31(3):426–428. doi:10.1021/ac60147a030

Mittal AK, Chisti Y, Banerjee UC (2013) Synthesis of metallic nanoparticles using plant extracts. Biotechnol Adv 31(2):346–356. doi:10.1016/j.biotechadv.2013.01.003

Mishra RR, Prajapati S, Das J, Dangar TK, Das N, Thatoi H (2011) Reduction of selenite to red elemental selenium by moderately halotolerant *Bacillus megaterium* strains isolated from *Bhitarkanika mangrove* soil and characterization of reduced product. Chemosphere 84:1231–1237. doi:10.1016/j.chemosphere.2011.05.025

Moldes D, Rodríguez S, Cameselle C, Sanromán MA (2003) Study of the degradation of dyes by MnP of *Phanerochaete chrysosporium* produced in a fixed-bed bioreactor. Chemosphere 51:295–303. doi:10.1016/S0045-6535(02)00406-X

Moss MO, Badii F, Gibbs G (1987) Reduction of biselenite to elemental selenium by *Aspergillus parasiticus*. Trans Br Mycol Soc 89(4): 578–580. doi:10.1016/S0007-1536(87)80094-3

Mukherjee P, Ahmad A, Mandal D, Senapati S, Sainkar SR, Khan MI, Ramani R, Parischa R, Ajayakumar PV, Alam M, Sastry M, Kumar R (2001) Bioreduction of $AuCl_4^-$ ions by the fungus *Verticillium* sp. and surface trapping of the gold nanoparticles formed. Angew Chem Int Ed Engl 40:3585–3588. doi:10.1002/1521-3773(20011001)40:19<3585

Nguyen VNH, Amal R, Beydoun D (2005) Photocatalytic reduction of selenium ions using different TiO_2 photocatalysts. Chem Eng Sci 60(21):5759–5769. doi:10.1016/j.ces.2005.04.085

Oremland RS, Herbel MJ, Blum JS, Langley S, Beveridge TJ, Ajayan PM, Sutto T, Ellis AV (2004) Structural and spectral features of selenium nanospheres produced by Se-respiring bacteria. Appl Environ Microbiol 70:52–60. doi:10.1128/AEM.70.1.52-60.2004

Papagianni M (2004) Fungal morphology and metabolite production in submerged mycelial processes. Biotechnol Adv 22(3):189–259. doi:10.1016/j.biotechadv.2003.09.005

Pazouki M, Panda T (2000) Understanding the morphology of fungi. Bioprocess Eng 22:127–143. doi:10.1007/s004490050022

Prasad KS, Patel H, Patel T, Patel K, Selvaraj K (2013) Biosynthesis of Se nanoparticles and its effect on UV-induced DNA damage. Colloids Surf B: Biointerfaces 103:261–266. doi:10.1016/j.colsurfb.2012.10.029

Prosser JI (1995) Kinetics of filamentous growth and branching. In: Gow NAR, Gadd GM (eds) The growing fungus. Springer, The Netherlands, pp 301–318

Rajakumar G, Rahuman AA, Roopan SM, Khanna VG, Elango G, Kamaraj C, Zahir AA, Velayutham K (2012) Fungus-mediated biosynthesis and characterization of TiO_2 nanoparticles and their activity against pathogenic bacteria. Spectrochim Acta A 91:23–29. doi:10.1016/j.saa.2012.01.011

Ramadan SE, Razak AA, Yousseff YA, Sedky NM (1988) Selenium metabolism in a strain of *Fusarium*. Biol Trace Elem Res 18:161–170. doi:10.1007/BF02917500

Rasband WS (1997–2014) ImageJ. U.S. National Institutes of Health, Bethesda, Maryland, USA. http://imagej.nih.gov/ij/

Rayman MP (2012) Selenium and human health. Lancet 379:1256–1268. doi:10.1016/S0140-6736(11)61452-9

Sanghi R, Verma P, Puri S (2011) Enzymatic formation of gold nanoparticles using *Phanerochaete chrysosporium*. Adv Chem Eng Sci 1(3): 154–162. doi:10.4236/aces.2011.13023

Saraswathy A, Hallberg R (2005) Mycelial pellet formation by *Penicillium ochrochloron* species due to exposure to pyrene. Microbiol Res 160(4):375–383. doi:10.1016/j.micres.2005.03.001

Sarkar J, Dey P, Saha S, Acharya K (2011) Mycosynthesis of selenium nanoparticles. Micro Nano Lett 6(8):599–602. doi:10.1049/mnl.2011.0227

Sastry M, Ahmad A, Islam N, Kumar R (2003) Biosynthesis of metal nanoparticles using fungi and actinomycete. Curr Sci 85(2):162–170

Serafin-Muñoz AH, Kubachka K, Wrobel K, Gutierrez-Corona JF, Yathavakilla SKV, Caruso JA, Wrobel K (2006) Se-enriched mycelia of *Pleurotus ostreatus*: distribution of selenium in cell walls and cell membranes/cytosol. Agric Food Chem 54:3440–3444. doi:10.1021/jf052973u

Soda S, Ike M (2011) Characterization of *Pseudomonas stutzeri* NT-I capable of removing soluble selenium from the aqueous phase under aerobic conditions. J Biosci Bioeng 112(3):259–264. doi:10.1016/j.jbiosc.2011.05.012

Syed A, Ahmad A (2012) Extracellular biosynthesis of platinum nanoparticles using the fungus *Fusarium oxysporum*. Colloids Surf B: Biointerfaces 97:27–31. doi:10.1016/j.colsurfb.2012.03.026

Teodoro JS, Simõesa AM, Duarte FV, Rolo AP, Murdoch RC, Hussain SM, Palmeira CM (2011) Assessment of the toxicity of silver nanoparticles in vitro: a mitocohondrial perspective. Toxicol in Vitro 25(3):664–670. doi:10.1016/j.tiv.2011.01.004

Tien M, Kirk TK (1988) Lignin peroxidase of *Phanerochaete chrysosporium*. In: Wood WA, Kellogg ST (eds) Methods in enzymology. Biomass, part b: lignin, pectin and chitin, vol 161. Academic, San Diego, pp 238–249

Tran PA, Webster TJ (2011) Selenium nanoparticles inhibit *Staphylococcus aureus* growth. Int J Nanomedicine 6:1553–1558. doi:10.2147/IJN.S21729

Tweedie JW, Segel IH (1970) Specificity of transport processes for sulfur, selenium, and molybdenum anions by filamentous fungi. Biochim Biophys Acta 196(1):95–106. doi:10.1016/0005-2736(70)90170-7

Thongchul N, Yang ST (2003) Controlling filamentous fungal morphology by immobilization on a rotating fibrous matrix to enhance oxygen transfer and L(+)-lactic acid production by *Rhizopus oryzae*. In: Saha BC (ed) Fermentation process development. Oxford University Press, New York, pp 36–51, ACS Symposium Series 862

USHHS. United States Department for Health and Human Services (2003) Toxicological profile for selenium. Available at: http://www.atsdr.cdc.gov/toxprofiles/tp92.pdf. Accessed 05 Mar 2014

Van Cutsem J, Van Gerven F, Fransen J, Schrooten P, Janssen PA (1990) The in vitro antifungal activity of ketoconazole, zinc pyrithione, and selenium sulfide against *Pityrosporum* and their efficacy as a shampoo in the treatment of experimental pityrosporosis in guinea pigs. J Am Acad Dermatol 22(6 Pt 1):993–998. doi:10.1016/0190-9622(90)70140-D

Verma VC, Kharwar RN, Gange AC (2010) Biosynthesis of antimicrobial silver nanoparticles by the endophytic fungus *Aspergillus clavatus*. Nanomedicine 5:33–40. doi:10.2217/nnm.09.77

Vetchinkina E, Loshchinina E, Kursky V, Nikitina V (2013) Reduction of organic and inorganic selenium compounds by the edible medicinal basidiomycete *Lentinula edodes* and the accumulation of elemental selenium nanoparticles in its mycelium. J Micriobiol 51(6):829–835. doi:10.1007/s12275-013-2689-5

Vigneshwaran N, Kathe AA, Varadarajan PV, Nachane RP, Balasubramanya RH (2006) Biomimetics of silver nanoparticles by white rot fungus, *Phanerochaete chrysosporium*. Colloids Surf B: Biointerfaces 53:55–59. doi:10.1016/j.colsurfb.2006.07.014

Vigneshwaran N, Ashtaputre NM, Varadarajan PV, Nachane RP, Paralikar KM, Balasubramanya RH (2007) Biological synthesis of silver nanoparticles using the fungus *Aspergillus flavus*. Mater Lett 61:1413–1418. doi:10.1016/j.matlet.2006.07.042

Wang C, Sun H, Li J, Li Y, Zhang Q (2009) Enzyme activities during degradation of polycyclic aromatic hydrocarbons by white rot fungus *Phanerochaete chrysosporium* in soils. Chemosphere 77:733–738. doi:10.1016/j.chemosphere.2009.08.028

Wang T, Yang L, Zhang B, Liu J (2010) Extracellular biosynthesis and transformation of selenium nanoparticles and application in H_2O_2 biosensor. Colloids Surf B: Biointerfaces 80(1):94–102. doi:10.1016/j.colsurfb.2010.05.041

Xu P, Liu L, Zeng G, Huang D, Lai C, Zhao M, Huang C, Li N, Wei Z, Wu H, Zhang C, Lai M, He Y (2014) Heavy metal-induced glutathione accumulation and its role in heavy metal detoxification in *Phanerochaete chrysosporium*. Appl Microbiol Biotechnol 98:6409–6418. doi:10.1007/s00253-014-5667-x

Zelmanov G, Semiat R (2013) Selenium removal from water and its recovery using iron (Fe^{3+}) oxide/hydroxide-based nanoparticles sol (NanoFe) as an adsorbent. Sep Purif Technol 103:167–172. doi:10.1016/j.seppur.2012.10.037

Zhang J, Wang H, Yan X, Zhang L (2005) Comparison of short-term *toxicity* between Nano-Se and selenite in mice. Life Sci 76:1099–1109. doi:10.1016/j.lfs.2004.08.015

Zhang J, Wang X, Xu T (2008) Elemental selenium at nano size (Nano-Se) as a potential chemopreventive agent with reduced risk of selenium toxicity: comparison with SE-methylselenocysteine in mice. Toxicol Sci 101(1):22–31. doi:10.1093/toxsci/kfm221

Zhang W, Chen Z, Liu H, Zhang L, Gao P, Li D (2011) Biosynthesis and structural characteristics of selenium nanoparticles by *Pseudomonas alcaliphila*. Colloids Surf B: Biointerfaces 88(1):196–201. doi:10.1093/toxsci/kfm221

Zieve R, Ansell PJ, Young TWK, Peterson PJ (1985) Selenium volatilization by *Mortierella* species. Trans Br Mycol Soc 84:177–179. doi:10.1016/S0007-1536(85)80240-0